*Journal of Chromatography*, 566 (1991) 309–326
*Biomedical Applications*
Elsevier Science Publishers B.V., Amsterdam

CHROMBIO. 5805

## Review

# Construction of kinetic models to understand metabolism *in vivo*

BARBARA E. WRIGHT

*Division of Biological Sciences, University of Montana, Missoula, MT 59812 (U.S.A.)*

ABSTRACT

This review describes increasingly complex kinetic models that simulate carbohydrate metabolism in a simple eucaryotic system which undergoes differentiation. Dynamic models of complex metabolic networks serve to organize and analyze the many interdependent variables involves and to define the rate-limiting events controlling metabolism *in vivo*. Since the ultimate justification for and test of any model are its predictive values, a series of predictions and related experiments will be described.

ABBREVIATIONS

UDPG, uridine diphosphoglucose; G6P, glucose-6-phosphate; G1P, glucose-1-phosphate; 6PG, 6-phosphoglucanate; R5P, ribose-5-phosphate; muco poly, mucopolysaccharide; F6P, fructose-6-phosphate; UTP, uridine triphosphate; GLY, glycogen; TRE, trehalose; GLU, glucose; MAL, malate; CIT, citrate; ACE, acetate; OAA, oxaloacetate; ST, stalk cells; EXT, external pool; PYR, pyruvate; DHAP, dihydoxyacetone phosphate; M6P, mannose-6-phosphate; GA3P, glyceraldehyde-3-phosphate; E4P, erythrose-4-phosphate; S7P, sedoheptulose-7-phosphate; Ru5P, ribulose-5-phosphate; SUC, succinate; F16DP, fructose 1, 6-diphosphate; EXGLU, exogenous glucose; AMP, adenosine monophosphate; ADP, adenosine diphosphate; UMP, uridine monophosphate; FUM, fumante; 2KG, 2 ketoglutanate; ACO, acetyl Co A; PROT, protein; ASP, aspartate; ALA, alanine.

## INTRODUCTION

I believe that many biochemists think that models incorporating enzyme data are not realistic: that not much has been learned from them, they are too theoretical, and that we do not really know enough as yet to make useful models of this kind. I hope to convince you that we do have the data and expertise to construct

0378-4347/91/$03.50 

and profit from such models, but only if we follow certain rules and only if our models have predictive value. Certainly it is very important to attempt to determine the extent to which the enormous amount of enzyme data we have collected from dead cells applies to living cells. The point, of course, is not to play games with mathematics and models but to use them as tools for understanding the dynamics of metabolism in living cells. Too often a model is made to fit a particular data-set but never challenged by further experiments to test the assumptions involved; too often a model is made to work by the arbitrary selection of input data or by making unjustified changes in model configuration. The reductionistic approach must get the credit for bringing biochemistry where it is today, but, as we all know, the living cell is an extremely complex system of inter-dependent sub-systems. A dynamic systems analysis will eventually be essential to understand the complexity involved. We must ask the extent to which our *in vitro* reaction rates, enzyme activities, kinetic mechanisms, and metabolite concentrations actually apply to circumstances existing *in vivo*. The ultimate test of our understanding is to use such data in dynamic models which demonstrate predictive value.

One of the most important kinds of information required for the construction of kinetic models is metabolite flux, obtained from tracer studies and the specific radioactivities of isolated metabolites. As will become evident, high-performance liquid chromatography (HPLC) is an indispensable technique in the purification of these metabolities to homogeneity.

The experimental system we have been using is *Dictyostelium discoideum*, which, under starvation conditions, differentiates from an amoeba into a fruiting body with stalk and spore cells. The fascinating life cycle of this cellular slime mold is depicted along the time axis of Fig. 1. In the presence of external nutri-

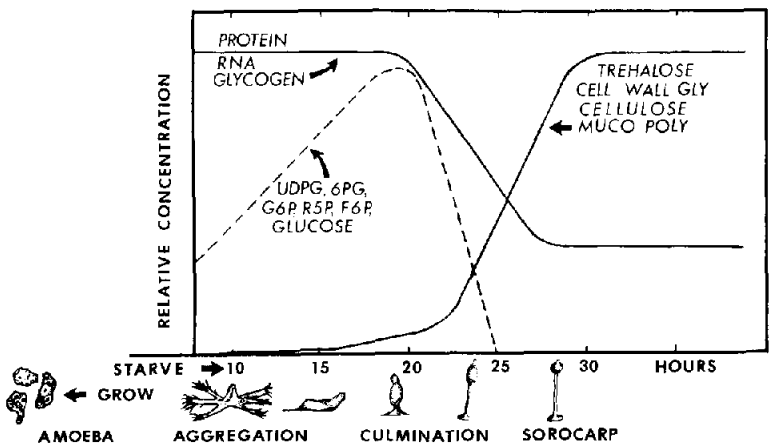


Fig. 1. Pattern of utilization and accumulation of endogenous metabolites and end-products during differentiation of *Dictyostelium discoideum*. Successive stages of the life cycle are depicted along the time axis.

ents, the organism grows and multiplies as free-living single amoebae. Under starvation conditions, growth ceases and the amoebae aggregate to form a multicellular colony which differentiates through several distinctive stages to form a sorocarp composed of stalk cells, which die, and spore cells, which will give rise to amoebae under appropriate conditions. During differentiation there is no net loss of carbohydrate. At aggregation most of the carbohydrate material is present as glycogen and RNA-pentose. In the middle of differentiation there occurs a transient accumulation of metabolites such as glucose-6-phosphate (G6P), 6-phosphogluconate (6PG), and UDP-glucose (UDPG). UDPG is the precursor for soluble glycogen and for all the end-product saccharides. At the end of development there is a decrease in glycogen and RNA and a comparable increase in new polysaccharide end products (trehalose, cellulose–glycogen cell wall complex, and mucopolysaccharide). Endogenous protein serves as the energy source in this system [1–4].

In the early 1960s we tried to make sense out of changes in the activities of various enzymes in extracts prepared at successive times over the course of differentiation in *Dictyostelium*. We ran into a number of artifacts, such as enzyme instability in these extracts, due to proteolysis, the presence or absence of inhibitors, activators, or stabilizing substrates. Moreover, these artifacts were often present early in differentiation but not later; thus, an enzyme could be inactivated

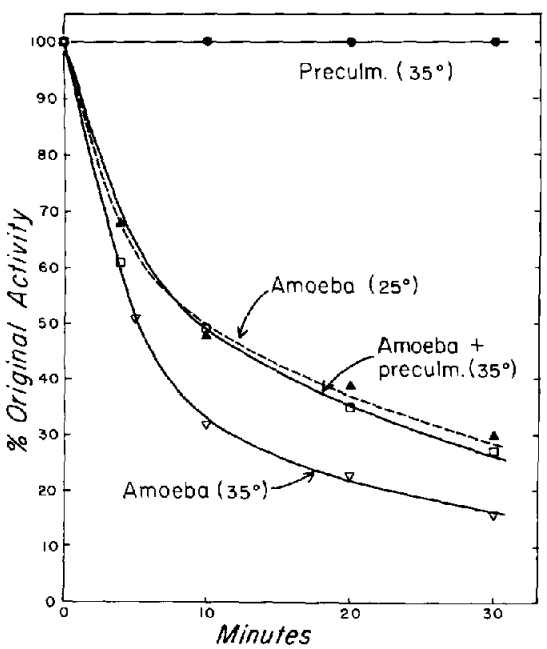


Fig. 2. Stability of UDP-glucose pyrophosphorylase as a function of time and temperature in extracts prepared at the amoeba and preculmination stages of differentiation [5].

quickly in extracts of amoebae and be quite stable in extracts prepared later in development. This was observed for a number of enzymes, including UDPG pyrophosphorylase. In Fig. 2 we see that the enzyme in amoebae extracts loses activity rapidly at 35 or 25°C. The enzyme is stable at 35°C in extracts prepared at preculmination; however, if the enzyme in preculmination extracts is mixed with amoeba extracts, it is inactivated by the proteolytic activity present in amoeba extracts [5]. Based on enzyme assays in crude extracts, it would apear as though the amount of enzyme increased more than twenty times during differentiation. Actually, no significant increase occurs in the amount of this enzyme [6]. In another case, enzyme activity was stable and constant in extracts prepared at all stages of development, but tracer studies showed that the rate of the reaction *in vivo* increased seven times; this turned out to be due simply to the accumulation of the substrate *in vivo* during development [7]. In another case, an end-product inhibitor accumulated to peak concentration at the end of differentiation, resulting in minimum enzyme activity *in vivo* when activity *in vitro* was maximum, as the inhibitor had been diluted [8]. Thus, enzyme activities *in vitro* were less than helpful in understanding the biochemical basis of differentiation in this system.

It soon became clear that in order to understand metabolism *in vivo* it was essential to know more about the behavior of metabolites and to know the rates of critical reactions *in vivo*. As shown in Fig. 3, we determined the rate of UDPG synthesis under steady state conditions, by exposing cells to [$^{14}$C]uracil and isolating UTP and UDPG to determine their specific radioactivities (S.R.). Thus, we could determine the rate of UDPG turnover, expressed in terms of cell volume [9]. It increased three-fold, from 0.08 to 0.24 m$M$/min between aggregation and cul-

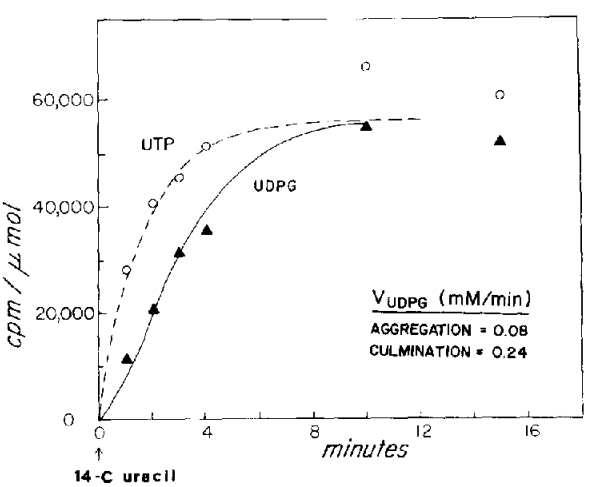


Fig. 3. Determination *in vivo* of UDP-glucose turnover at aggregation and culmination. Cells were exposed to [$^{14}$C]uracil under steady state conditions to determine the S.R. of UTP and UDPG as a function of time [9].

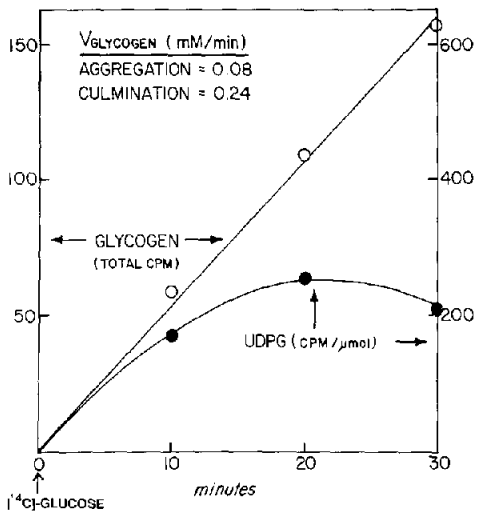


Fig. 4. Determination of the rate of glycogen synthesis *in vivo* under steady state conditions at aggregation and at culmination. Cells were exposed to [$^{14}$C]glucose to determine the S.R. of UDPG and the rate of increase in total counts in glycogen [10].

mination. Another *in vivo* flux study was to expose cells to [$^{14}$C]glucose and relate the increase in total counts in glycogen to the S.R. of the precursor, UDPG [10]. In Fig. 4 the rate was again 0.08 m$M$/min at aggregation and 0.24 m$M$/min at culmination. Similar analyses were done for cellulose [9] and trehalose [11] synthesis; the latter one is shown in Fig. 5. Again, we related the increase in counts in the trehalose pool to UDPG S.R. Over the approximate 7-h period of trehalose accumulation the rate of synthesis averaged about 0.02 m$M$/min. This value was also calculated based on actual measurements of trehalose accumulation, indicating that trehalose does not turn over and that the UDPG isolated in the tracer studies was the actual physiological precursor pool. This was directly demonstrated years later [12].

Metabolite perturbation studies have been very important in testing predictions of our models. Fig. 6 shows a steady state model of carbohydrate metabolism, with the lower portion representing stalk cells and the upper portion spore cells [13]. As I have just explained, the fluxes of many of these reactions were determined independently: trehalose and cellulose synthesis, and the turnover of glycogen and UDPG. We knew flux through the citric acid cycle (CAC) based on $O_2$ consumption, and have separated very detailed models of the CAC based on tracer studies using radioactive amino acids [2,3]. The box at the top of the figure describes a 90-min perturbation experiment using 50.0 m$M$ glucose or ribose-5-phosphate (RIB-5-P). Glucose stimulates both G6P and glycogen levels, while RIB-5-P affects only G6P levels. This observation and many others led us to conclude that there were three glycogen pools: one in spore cells that is only

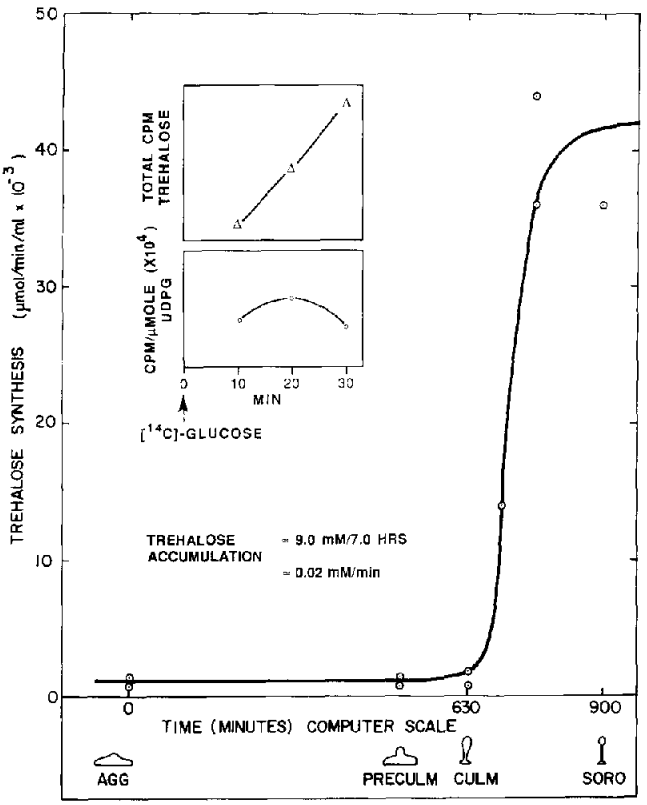


Fig. 5. Rate of trehalose synthesis *in vivo* at various stages of development [11]. Cells are exposed to [$^{14}$C]glucose to relate the increase in total counts in the trehalose pool to the S.R. of UDPG. See text for further details.

degraded, one in stalk cells that is only degraded, and one in spore cells which is both synthesized and degraded. There is a limited, vestigial kind of metabolism in the stalk cells, which are dying and highly permeable. Thus RIB-5-P permeated only the stalk cells and enhanced G6P levels. Glucose entered both cell types; as glycogen is synthesized only in spore cells, both G6P and glycogen levels increased.

Using a computer program called TFLUX, we could obtain a "flux map" of all the pathways indicated here [14]. Input for the TFLUX program consists of compartmented metabolite concentrations, the rate of each reaction and the S.R. of the tracer [$^{14}$C]glucose. The output is the S.R. of each metabolite as a function of time, which should match the experimental data. Simulation of our data required the existence of two pools of G6P, G1P, and glucose. Experimentally, we exposed the organisms to [$^{14}$C]glucose and, at 20-min intervals, isolated all these metabolites to determine their S.R.s [13]. It is of course critical that they be purified to homogeneity to obtain correct S.R.s on which to base our flux map.

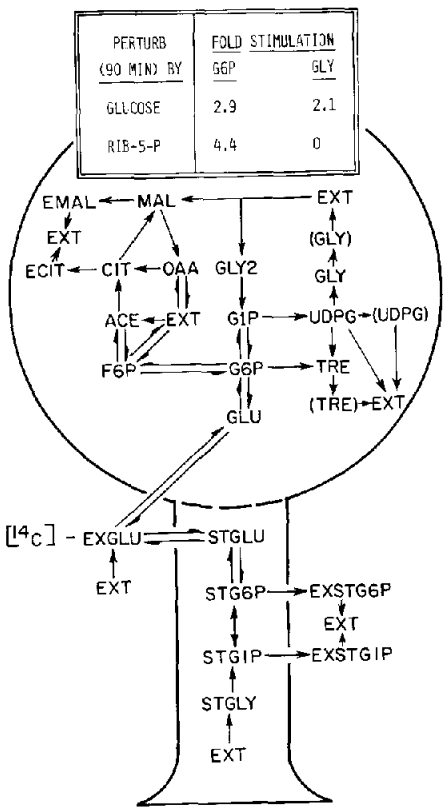


Fig. 6. Steady state model of carbohydrate metabolism in spore and stalk cells of *Dictyostelium discoideum* [13]. The insert (box) summarizes a perturbation experiment in which G6P and glycogen levels were enhanced by exogenous glucose or ribose-5-phosphate.

After preparing cell-free extracts, the first purification step is to use a borate column, shown in Fig. 7; an ammonium borate gradient is followed by one of sodium chloride. After this initial separation, a variety of paper chromatographic steps are employed, depending upon which metabolites are to be separated. Alkaline phosphatase is used to convert the sugar phosphates to free sugars, followed by their separation by HPLC. At each step metabolites are counted and assayed enzymatically until constant S.R. is achieved. A charcoal step is included for the isolation of UDPG. In Fig. 8 is shown the separation of some of the sugars by HPLC. In Fig. 9 is shown the match between computer output curves and data points for the model in Fig. 6 [13]. The word MIX refers to the average S.R. of the spore and stalk cell pools, which mix on cell rupture. Of course, all these metabolite S.R.s are interdependent, and must be compatible, putting severe constraints on the model. For example, we know that UDPG is a single pool in spore cells, and that G1P is its immediate precursor. Since the S.R. of UDPG is higher than that of G1P there must be two pools of G1P, one of which parallels the S.R. of

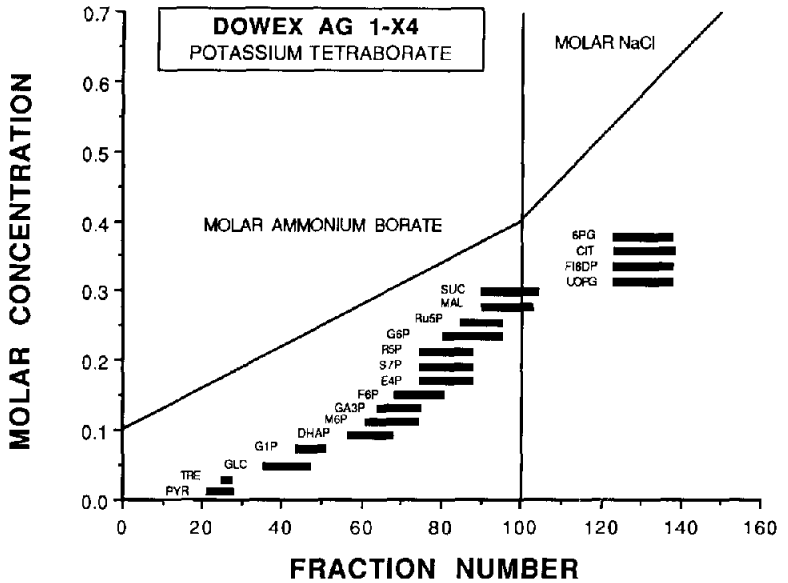


Fig. 7. Separation of metabolites on a borate column using an ammonium borate gradient followed by one of sodium chloride.

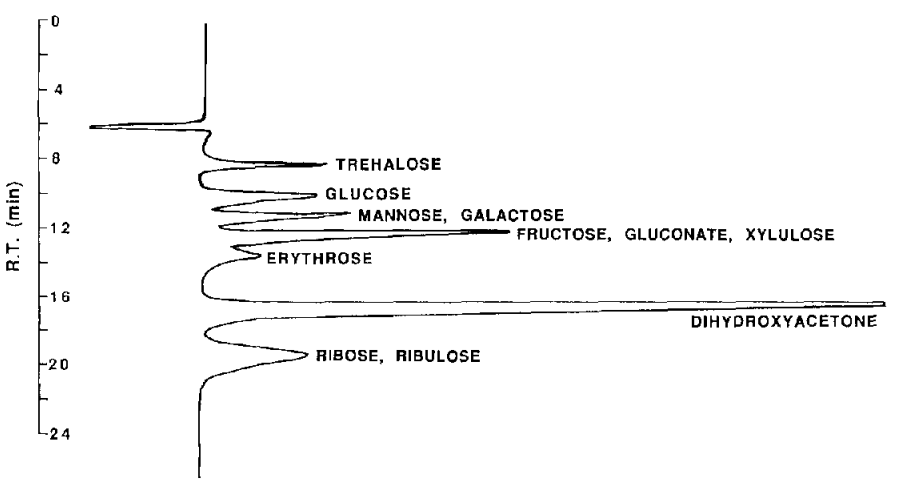


Fig. 8. Separation by HPLC of some free sugars obtained from sugar phosphates by treatment with alkaline phosphatase. Column: Re7ex RHM-monosaccharide, $H^+$ form. Solvent: 0.01 $M$ $(NH_4)_2SO_4$ at 0.6 ml/min. Temperature: 23°C. UV detector: 193 mm. Amount of sugars: 50–100 mmol.

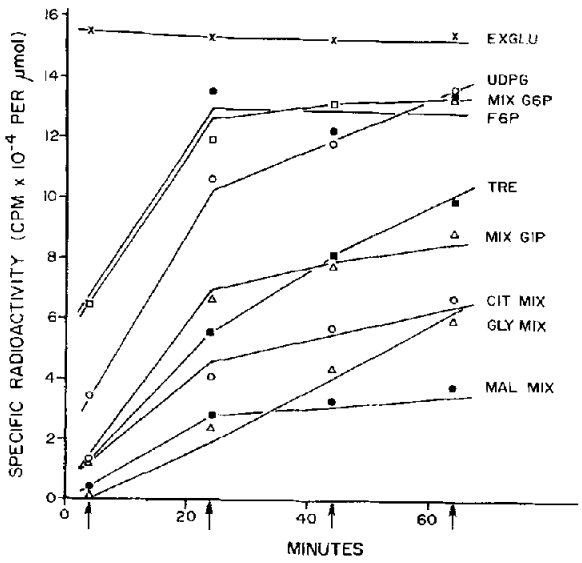


Fig. 9. Match between computer output (curves) and data points for one of the steady state models [13].

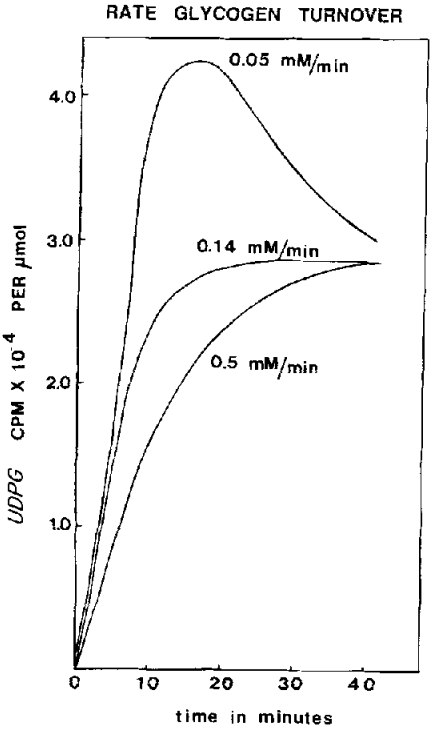


Fig. 10. Simulations indicating the shape of the UDPG S.R. curve, assuming three different rates of glycogen turnover [15]. See text for futher details.

UDPG in spore cells. By difference, we can deduce the S.R. curve for the stalk cell G1P. Another criterion for judging the fit of the model to the data is the shape of the UDPG curve [15]. In Fig. 10 we have assumed different rates of turnover for the spore glycogen pool. At 40 min, all curves have the same value, but only the middle curve also closely simulates the correct shape of the UDPG curve. We therefore concluded that the rate of glycogen turnover was approximately 0.14 m$M$/min.

## RESULTS AND DISCUSSION

Now I shall turn to a discussion of our transition models, using a computer program called METASIM [16]. These models simulate changes in metabolism as a function of time. They incorporate the results of the steady state TFLUX analyses and also have enzyme mechanisms in them. Fig. 11 shows our first simple transition model, depicting the glycogen cycle [17]. We had determined

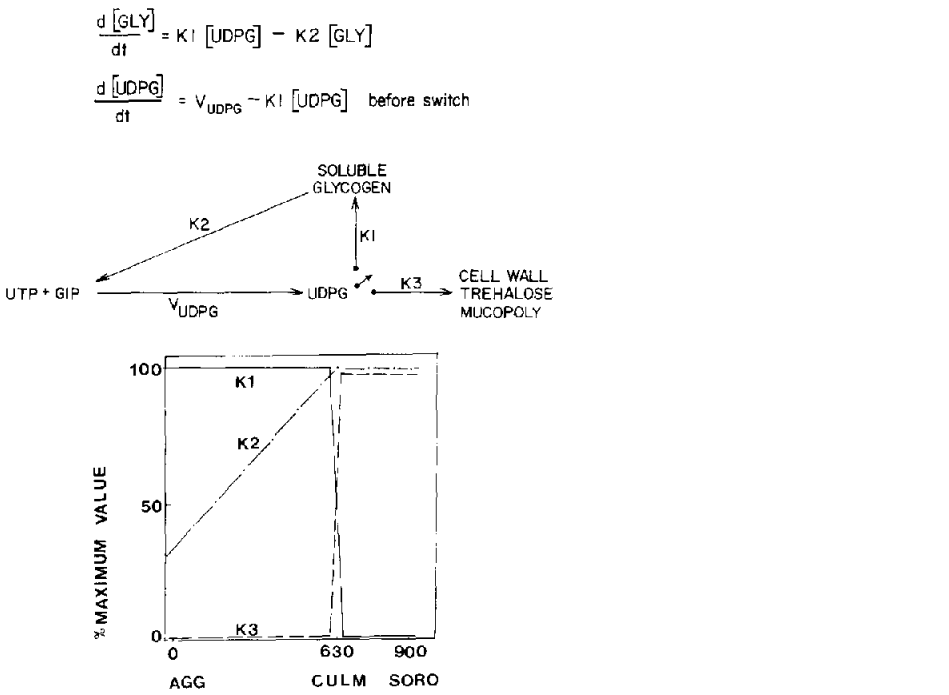


Fig. 11. First transition model of carbohydrate metabolism in *Dictyostelium discoideum* [17]. Two of the seven differential equations describing this model are shown above it, and the behavior of the three rate constants are shown below the model. See text for details.

$V_{UDPG}$ (Fig. 3), the concentrations of UTP, G1P, UDPG and glycogen, and the $K_m$ values for these substrates. Using the following simple kinetic expression

$$V_{UDPG} = V_{max}\left(\frac{1}{\frac{K_{UTP}}{[UTP]} + 1}\right)\left(\frac{1}{\frac{K_{G1P}}{[G1P]} + 1}\right)$$

(where $K_{UTP}$ and $K_{G1P}$ are $K_m$ values for UTP and G1P and [UTP] and [G1P] are concentrations of UTP and G1P, respectively) $V_{max}$ was calculated as the only unknown because, as I explained earlier, we did not believe that *in vitro* enzyme activities were very relevant to reaction rates *in vivo*. We now call this calculated value $V_{VIVO}$ [18]. I shall say more about it later.

This first simple model was very exciting because it revealed so much and made so many testable predictions. We had to express all metabolite pools in glucose equivalents to make the model, and thereby we discovered that the decrease in glycogen at the end of differentiation could almost account for the increase in the amount of new end products! That is one outcome of making models: in their logic and consistency they often force us to see relationships we had previously ignored. Knowing $V_{UDPG}$ and the concentration of all metabolite pools, $K_1$ and $K_2$ could be calculated, assuming that a steady state exists and assuming that, initially, UDPG is used only for glycogen synthesis. To make the model simulate the data, only two changes had to be made: First, UDPG was used only for glycogen synthesis in the glycogen cycle until the middle of development; then $K_1$

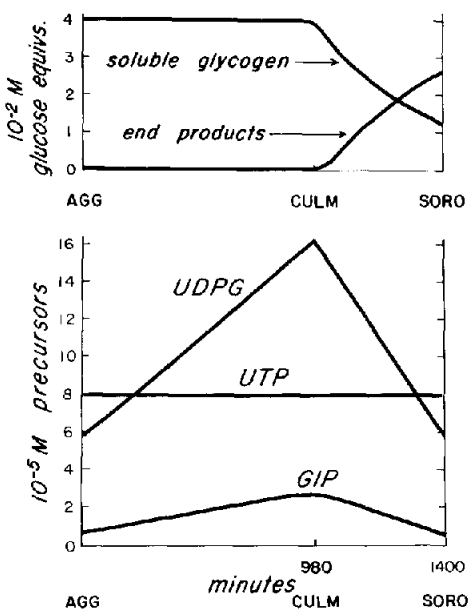


Fig. 12. Simulations based on the model (Fig. 11) which match the data [17].

went to zero and $K_3$ took its value, as indicated in the lower figure. Second, $K_2$ (representing glycogen phosphorylase) increased three times from the beginning to the middle of differentiation. Only seven simple equations describe this model; two are shown above the model. Fig. 12 shows the model output which matches the observed changes in metabolite concentrations. Although it is not shown here, the model also simulates the fact that the rate of UDPG synthesis increases three-fold, due to increased G1P levels, which are due to the three-fold increase in glycogen phosphorylase activity. Here are the predictions made by this model; all of them have been substantiated [1].

(1) The rates of glycogen, cellulose, and trehalose synthesis are directly proportional to the concentration of UDPG. All of these enzymes have since been characterized *in vitro*, and their $K_m$ values for UDPG are much higher than the physiological concentration of UDPG.

(2) The rates of glycogen and G1P synthesis equal the rate of UDPG synthesis at aggregation and increase three-fold by culmination. After this prediction was made, the rate of glycogen turnover *in vivo* was examined (Fig. 4). At aggregation, it was found to be the same as UDPG synthesis (Fig. 3), and to increase three-fold by the culmination stage of development.

(3) Glycogen phosphorylase is rate-limiting to G1P (and therefore also UDPG) synthesis; it must increase in activity during differentiation. This enzyme was later purified to homogeneity, and immunological studies demonstrated that it did increase significantly in concentration during differentiation [19,20].

(4) UDPG pyrophosphorylase is not rate-limiting for UDPG synthesis; if it increases in activity during differentiation it must also be inhibited, or G1P would not accumulate. It was later found that pyrophosphorylase mutants with a fraction of the normal level of this enzyme develop quite normally [21,22]. It was also found that UDPG inhibits the enzyme at physiological levels [23]. Moreover, simulations indicated that, because of the "kinetic position" of this enzyme, increasing its activity results in a compensatory decrease in the steady state level of G1P, rather than an increase in the rate of the reaction [17]. Thus, UDPG pyrophosphorylase is not rate-controlling under steady stae conditions *in vivo*.

Fig. 13 indicates the areas of metabolism for which we now have transition models, which simulate changes in flux and metabolite concentrations during differentiation. Actually, these were analyzed as four different models: carbohydrate metabolism in spore cells and in stalk cells (double boxes), pentose metabolism and the citric acid cycle. Ninety percent of he approximately 300 parameters composing these models are experimental data. The rates of the reactions have been determined *in vivo*, for the most part with radioactive tracers; enzymes have been purified and kinetic mechanisms and constants determined for all the reactions which are encircled. The double boxes represent stalk cell metabolites and the broken boxes exogenous metabolites which have been used at high levels to perturb the organism and the model to test various assumptions and to make predictions. These models integrate and simulate approximately 55 established

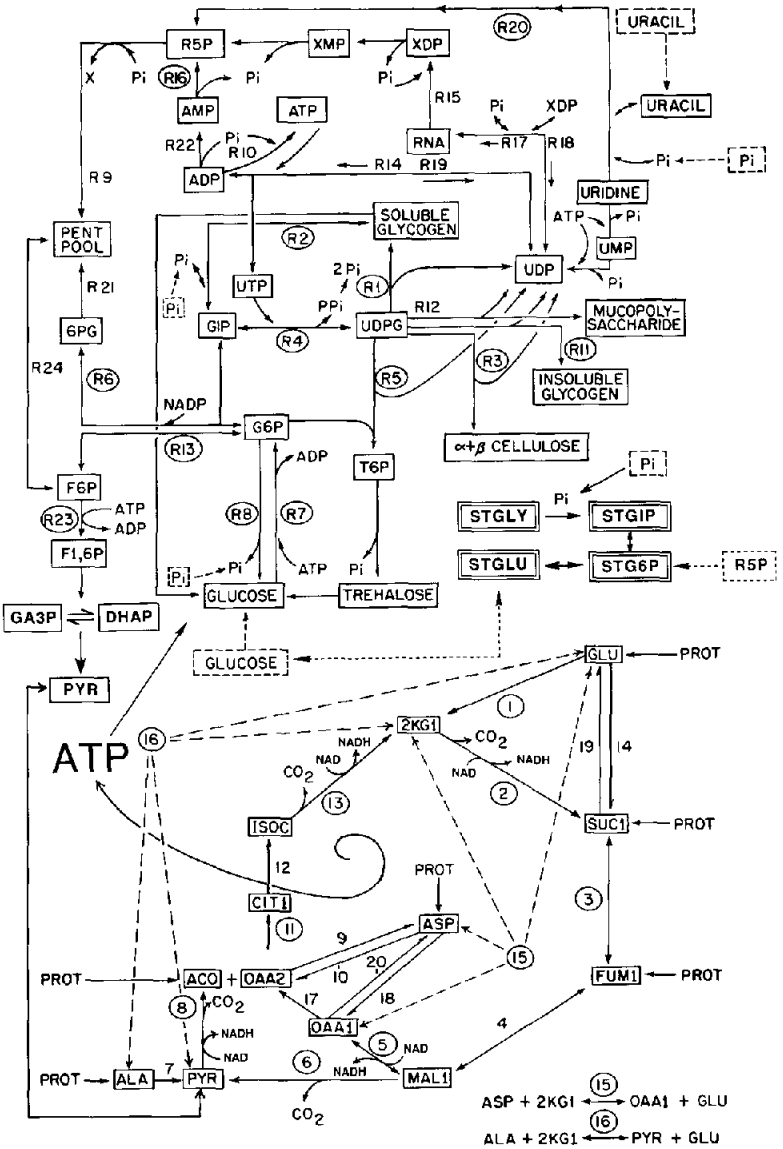


Fig. 13. Metabolic pathways in *Dictyostelium* for which there are transition models. See text for details.

reactions and flux patterns, 100 metabolite accumulation profiles for normal and perturbed metabolism, 25 enzyme mechanisms and 75 kinetic constants. The differential equations describing each reaction are solved simultaneously and output from the models consist of reaction rates and metabolite concentrations as a function of time. Thus we have identified over 180 substrates, products, effectors, and enzymes controlling these reactions, all of which are essential to biochemical differentiation in this organism. We also know which enzymes are rate-control-

ling. We believe the models reflect many aspects of metabolism *in vivo* because predictive value frequently has been demonstrated. Thus far 36 of 40 predictions tested have been substantiated. I have described four, and will briefly describe three more, two of which were substantiated unknowingly in other laboratories.

In 1975 we published a paper in which we made "computer mutants". That is, we varied the activities of five of these enzymes in the model to predict the effects on metabolite levels [24]. A two-fold increase in glycogen phosphorylase resulted in specific increases in trehalose (four-fold), G6P (three-fold), UDPG (two-fold), and very little increase in cellulose. While this manuscript was in press a paper from England appeared describing a variant of *Dictyostelium* which actually had this pattern of increase in metabolite levels [25]. The authors could not understand the metabolic basis for these changes, especially as trehalose levels increased the most, four-fold, yet no increase in trehalose-6-phosphate (T6P) synthase activity was detected. Although they noted that glycogen phosphorylase happened to be twice as active in their variant, they did not relate this fact to the change in pattern of metabolite levels. We knew, of course, that it could fully account for their observations. Had an increase in T6P synthase activity been detected, we would have predicted that it could not occur *in vivo*, as that would be incompatible with the accumulation of the two precursors, G6P and UDPG.

As a result of exploring this area of the model we made another prediction, namely, that perturbing the organism or the model with an external source of

**PREDICTIONS:**

1) GLUCOSE PULSE WILL INCREASE TRE/CELL RATIO
2) GLUCOSE POOL 1/20 [CELL] MUST EXIST

| | CONCENTRATION (mM) | | | |
|---|---|---|---|---|
| | TOTAL | GLY | TRE | CELL |
| NO GLUCOSE | | | | |
| EXPERIMENT | 99 | 16 | 8 | 35 |
| MODEL | 96 | 19 | 8 | 30 |
| PLUS GLUCOSE | | | | |
| EXPERIMENT | 206 | 96 | 40 | 37 |
| MODEL | 215 | 100 | 37 | 38 |

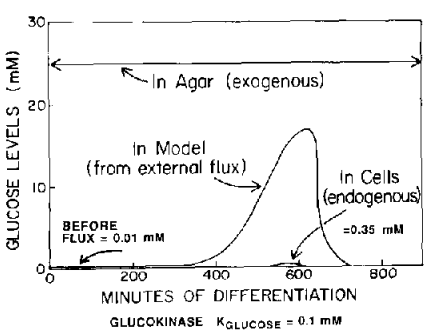


Fig. 14. Table: Comparison of experimental and model values for the effect of imposing external glucose on the organism or the model. Figure: Comparison of glucose levels measured experimentally or observed in the model before and after a pulse of external glucose [26]. See text for details.

glucose should also increase the trehalose/cellulose ratio by preferentially enhancing trehalose levels. In other words, increasing the hexose phosphate levels by stimulating the glucokinase reaction should have a similar effect to increasing glycogen phosphorylase activity. As shown in Fig. 14, such an effect was then demonstrated experimentally [26]: exogenous glucose increased the trehalose/cellulose ratio four-to five-fold, by selectively increasing trehalose levels from 8 to 40 m$M$. Glycogen levels also increased, about six-fold. Clearly, the rate of G6P formation was stimulated. However, the measured level of cellular glucose was 0.35 m$M$, and the $K_m$ of the enzyme for glucose was 0.1 m$M$ [27]. As the enzyme was saturated, more glucose could not achieve the observed experimental result. We concluded that the substrate/$K_m$ ratio must in fact be lower *in vivo*, due to some form of compartmentation or to other circumstances. The substrate/$K_m$ ratio was therefore decreased in the model by lowering the glucose level 35-fold, to 0.01 m$M$. Under these conditions, a pulse of external glucose on the model could increase the rate of the glucokinase reaction and simulate the data (Fig. 14). These results in turn led to another prediction, namely, that the cellular glucose pool being affected or expanded by exogenous glucose must be at least twenty times smaller than the average cellular level of 0.35 m$M$. Unaware of our results and predictions, Wilson and Rutherford [28] were analyzing glucose and trehalose levels in the spore and stalk cells of *Dictyostelium*. As shown in Fig. 15, they found that spore glucose levels were undetectable ($<0.08$ m$M$), while stalk glucose levels were extremely high, accounting for virtually all of the glucose mea-

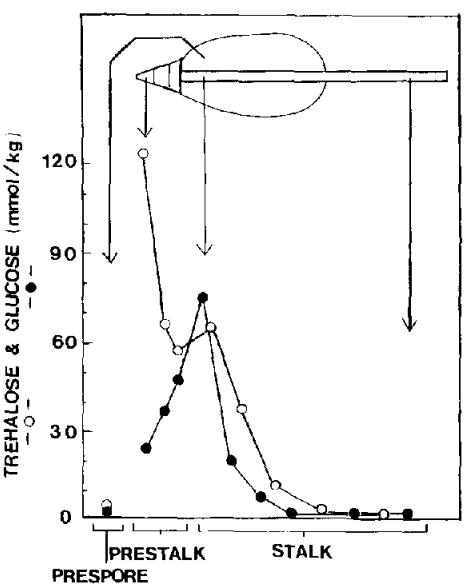


Fig. 15. Glucose and trehalose levels in the spore and stalk cells of a young sorocarp of *Dictyostelium discoideum* (taken from Wilson and Rutherford [28]).

sured in culmination extracts. Thus, it was the low-level spore glucose pool that was expanded by external glucose! This made sense, because the stalk cells were dying, and glycogen was only synthesized in the spore cells.

I will conclude by making a general prediction about enzyme activities in vivo. As you may recall, we calculate enzyme activities for our transition models, rather than use *in vitro* data. Appropriate enzyme kinetic mechanisms and constants describe each reaction in these models. Most are very complicated equations, but I can use the following simple expression to illustrate what we do:

$$\text{rate} = V_{\max}(A/K_A + A)$$

where $A$ = substrate concentration and $K_A = K_m$ value for A. We know the rate of each reaction from *in vivo* tracer studies; we also know the $K_m$ and substrate concentration. Thus we can calculate enzyme activity, which we call $V_{vivo}$ to distinguish it from $V_{max}$, which has been determined from *in vitro* data for all the enzymes.

TABLE 1

COMPARISON OF REACTION RATES DETERMINED *IN VIVO* WITH RATES CALCULATED FROM $V_{max}$ VALUES MEASURED WITH THE ISOLATED ENZYMES

Taken from ref. 18 with permission.

| Enzyme | Rate *in vivo* | Calculated rate | Ratio |
|---|---|---|---|
| Isocitrate dehydrogenase | 2.20 | 0.04 | 0.02 |
| Glutamate dehydrogenase | 0.38 | 0.98 | 2.6 |
| 2-Oxoglutarate dehydrogenase | 2.49 | 0.0014 | 0.00056 |
| Malic enzyme | 1.00 | 1.71 | 1.8 |
| Succinate dehydrogenase | 2.88 | 187.8 | 65.2 |
| Malate dehydrogenase | 2.01 | 12.4 | 6.2 |
| Citrate synthase | 2.20 | 145.7 | 66.2 |
| Pyruvate dehydrogenase | 1.64 | 0.0074 | 0.0045 |
| Aspartate transaminase | 0.18 | 0.48 | 2.7 |
| Alanine transaminase | 0.10 | −0.16 | 1.6 |
| Glycogen phosphorylase | −0.20 | −0.16 | 0.8 |
| Glucokinase | 0.01 | 0.08 | 8.0 |
| UDP-glucose pyrophosphorylase | 0.22 | 0.37 | 1.7 |
| Glycogen synthase | 0.13 | 0.83 | 6.4 |
| Trehalose 6-phosphate synthase | 0.009 | 0.01 | 1.1 |
| Glucose 6-phosphate dehydrogenase | 0.001 | 1.0 | 1000.0 |
| 6-Phosphogluconate dehydrogenase | 0.0009 | 0.009 | 10.0 |
| Phosphoglucose isomerase | 0.03 | 6.2 | 206.0 |
| Uridine phosphorylase | 0.01 | 0.35 | 35.0 |
| 5′-AMP nucleotidase | 0.02 | 2.4 | 120.0 |
| Glucose 6-phosphatase | 0.01 | 0.006 | 6.0 |
| Phosphofructokinase | 0.01 | 0.53 | 53.0 |
| Cell wall glycogen synthase | 0.02 | 0.006 | 0.3 |

In Table 1, we compare the experimentally determined rates of 23 reactions in our models to the rates calculated using $V_{max}$ values in each of the appropriate enzyme kinetic expressions. As I have stressed, many of these rates were determined individually *in vivo* with radioactive tracers; moreover they are all compatible within the models and represent very reliable data. Using $V_{max}$ values, the calculated rates are on average 30-fold higher than the measured *in vivo* rates. Two membrane-bound enzyme complexes, ketoglutarate dehydrogenase and pyruvate dehydrogenase, were not included in this average. They fall apart in the preparation of cell extracts and have very low recoveries. These are a number of possible explanations for observing excess enzyme *in vitro*. Protein is used as an energy source in this system. Due to the general vulnerability of most proteins to proteolytic attack, excessive enzyme protein concentrations may be essential in order to ensure adequate catalytic activity in times of starvation or stress. Another explanation may be that a large fraction of enzyme activity assayed *in vitro* in dilute solution is actually inactive *in vivo*, or unavailable to substrate, due to enzyme-bound product or inhibitor. For example, in muscle, a substantial part of glyceraldehyde-3-posphate dehydrogenase exists bound to 3-phosphoglycerate [29]. Enzymes have also been found to serve structural roles [30]. *In vitro*, of course, enzymes are diluted and assayed under optimal conditions of pH, coenzyme concentration, and so on, which probably do not apply *in vivo*. In any event, it is clear from this table that it would have been impossible to make a realistic model using $V_{max}$ values.

In conclusion, we believe the construction and analysis of these models has been essential to our understanding of the dynamics of metabolism in the living organism. Their predictive value demonstrates that in many respects they reflect reality. We have shown that *in vitro* enzyme activities cannot be used in realistic kinetic models of metabolism, but enzyme mechanisms and kinetic constants can be used. We know which enzymes and their genes are rate-controlling in this system; about one third of the enzymes in this network do not limit the rate of the reaction they catalyze. In any metabolic system, it is necessary to know which enzymes and metabolites are rate-controlling in order, for example, to select an inhibitor or a mutant affecting the accumulation of an important metabolite, such as cholesterol.

Every organism must have its own unique model, and all the data in the model should be derived from that organism. Moreover, to construct a realistic model with predictive value, the model should consist primarily of data. While this is no small task, an understanding of the complexities of metabolism in living cells is surely the most direct route to the identification of rate-limiting steps and, ultimately, to influencing the course of metabolism *in vivo*.

ACKNOWLEDGEMENT

This work was supported by Public Health Service Grant AG03884 from The National Institutes of Health.

REFERENCES

1 B. E. Wright and P. J. Kelly, *Curr. Topics Cell. Regul.*, 19 (1981) 103.
2 P. J. Kelly, J. K. Kelleher and B. E. Wright, *Biochem. J.*, 184 (1979) 581.
3 P. J. Kelly, J. K. Kelleher and B. E. Wright, *Biochem J.*, 184 (1979) 589.
4 J. K. Kelleher, P. J. Kelly and B. E. Wright, *J. Bacteriol.*, 138 (1979) 467.
5 B. E. Wright and D. Dahlberg, *J. Bact.*, 95 (1968) 983.
6 G. L. Gustafson, W. Y. Kong and B. E. Wright, *J. Biol. Chem.*, 248 (1973) 5188.
7 B. E. Wright and S. Bard, *Biochem. Biophys. Acta*, 71 (1963) 45.
8 K. Gezelius and B. E. Wright, *J. Gen. Microbiol.*, 38 (1965) 309.
9 R. G. Pannbacker, *Biochemistry*, 6 (1967) 1283.
10 R. Marshall, D. Sargent and B. E. Wright, *Biochemistry*, 9 (1970) 3087.
11 D. Sargent and B. E. Wright, *J. Biol. Chem.*, 246 (1971) 5340.
12 Y. Y. Chiew, J. M. Reimers and B. E. Wright, *J. Biol. Chem.*, 260 (1985) 15 325.
13 B. E. Wright and J. M. Reimers, *J. Biol. Chem.*, 263 (1988) 14906.
14 P. Sherwood, P. J. Kelly, J. K. Kelleher and B. E. Wright, *Comp. Prog. Biomed.*, 10 (1979) 66.
15 B. E. Wright, *J. Theor. Biol.*, 110 (1984) 445.
16 D. J. M. Park and B. E. Wright, *Comp. Prog. Biomed.*, 3 (1973) 10.
17 B. E. Wright, *J. Cell Physiol. Suppl. 1*, 71 (1968) 145.
18 B. E. Wright and K. R. Albe, in A. Cornish-Bowden (Editor), *Control of Metabolic Processes, NATO ASI Series*, Plenum Press, New York, 1990, Ch. 28, 317.
19 D. A. Thomas and B. E. Wright, *J. Biol. Chem.*, 251 (1976) 1253.
20 D. A. Thomas and B. E. Wright, *J. Biol. Chem.*, 251 (1976) 1258.
21 R. L. Diamond, P. A. Farnsworth and W. F. Loomis, *Dev. Biol.*, 50 (1976) 169.
22 D. J. Watts, *Biochem. J.*, 220 (1984) 1.
23 G. L. Gustafson and B. E. Wright, *Crit. Rev. Microbiol.*, 1 (1972) 453.
24 B. E. Wright and D. J. M. Park, *J. Biol. Chem.*, 250 (1975) 2219.
25 B. D. Hames and J. M. Ashworth, *Biochem. J.*, 142 (1974) 317.
26 B. E. Wright, A. Tai and K. A. Killick, *Eur. J. Biochem.*, 74 (1977) 217.
27 P. Baumann, *Biochemistry*, 8 (1969) 5011.
28 J. B. Wilson and C. L. Rutherford, *J. Cell. Physiol.*, 94 (1978) 37.
29 W. Bloch, R. A. MacQuarrie and S. A. Bernhard, *J. Biol. Chem.*, 246 (1971) 246.
30 G. J. Wistow, J. W. M. Mulders and W. W. de Jong, *Nature*, 326 (1987) 622.